

1       **Three Northern Regions Shelter Forest contributed to long-term**  
2       **increasing trend of biogenic isoprene emissions in Northern China**

3       **Authors:**

4       Xiaodong Zhang<sup>1</sup>, Tao Huang<sup>1\*</sup>, Leiming Zhang<sup>2</sup>, Yanjie Shen<sup>1</sup>, Yuan Zhao<sup>1</sup>, Hong Gao<sup>1</sup>,  
5       Xiaoxuan Mao<sup>1</sup>, Chenhui Jia<sup>1</sup>, Jianmin Ma<sup>1,3\*</sup>

6  
7       **Affiliation:**

8       <sup>1</sup>Key Laboratory for Environmental Pollution Prediction and Control, Gansu Province  
9       College of Earth and Environmental Sciences, Lanzhou University, Lanzhou 730000, P.  
10      R. China

11      <sup>2</sup>Air Quality Research Division, Environment Canada, Toronto, Ontario, M3H 5T4,  
12      Canada

13      <sup>3</sup>CAS Center for Excellence in Tibetan Plateau Earth Sciences, Beijing 100101, China  
14

15      \***Corresponding author:** Jianmin Ma, Tao Huang

16      Tel: +86 15293166921, fax: +86-931-8911843, email: [jianminma@lzu.edu.cn](mailto:jianminma@lzu.edu.cn);  
17      huangt@lzu.edu.cn

18  
19      **Abstract**

20      To assess the long-term trends of isoprene emissions in Northern China and the  
21      impact of the Three Northern Regions Shelter Forest (TNRSF) on these trends, a  
22      database of historical biogenic isoprene emissions from 1982 to 2010 was developed  
23      for this region using a biogenic emission model for gases and aerosols. The total  
24      amount of the biogenic isoprene emissions during the three decades was 4.4 Tg in  
25      Northern China and 1.6 Tg in the TNRSF, with annual emissions ranged from 132,000  
26      to 176,000 ton yr<sup>-1</sup> and from 45,000 to 70,000 ton yr<sup>-1</sup>, respectively, in the two regions.  
27      Isoprene emission fluxes have increased substantially in many places of the TNRSF  
28      over the last three decades due to the growing trees and vegetation coverage,  
29      especially in the Central-North China region where the highest emission incline

30 reached to 58% from 1982 to 2010. Biogenic isoprene emissions produced from  
31 anthropogenic forests tended to surpass those produced from natural forests, such as  
32 boreal forests in Northeastern China. The estimated isoprene emissions suggest that  
33 the TNRSF has altered the long-term emission trend in North China from a decreasing  
34 trend during 1982 to 2010 (slope=-0.533,  $R^2=0.05$ ) to an increasing trend for the same  
35 period of time (slope=0.347,  $R^2=0.014$ ), providing strong evidence for the change in  
36 the emissions of biogenic volatile organic compounds (BVOCs) induced by the  
37 human activities on decadal or longer time scales.

38 **Key words:** Volatile organic compounds, human activities, biogenic emissions,  
39 statistical trend

## 40 **1. Introduction**

41 While trees and plants can efficiently remove pollutants from the atmosphere (Nowak  
42 et al., 2006, 2014; Myles et al., 2012; Camporn, 2013; Fenn et al., 2013; Adon et al.,  
43 2013; Zhang et al., 2015), they also contribute to air pollution through atmospheric  
44 chemistry. It has been widely acknowledged that terrestrial ecosystems release large  
45 quantities of reactive biogenic volatile organic compounds (BVOCs) into the  
46 atmosphere as a significant product of biosynthetic activities of trees and plants  
47 (Purves et al., 2004; Zemankova and Brechler, 2010). BVOCs play important roles in  
48 tropospheric chemistry, carbon budget, and global climate change (Purves et al., 2004;  
49 Nichol and Wong, 2011; Aydin et al., 2014). For example, BVOCs are precursors of  
50 surface ozone formation in the presence of nitrogen oxide ( $\text{NO}_x$ ) (Penuelas et al.,  
51 2009; Penuelas and Staudt, 2010). It has been shown that VOC emissions from

52 biogenic sources have far exceeded those from anthropogenic sources (Guenther et al.,  
53 1994, 1995; Aydin et al., 2014).

54 Among the three dominant VOCs (isoprene, monoterpenes, oxygenated  
55 compounds) contributing to BVOC emission fluxes, isoprene accounts for 70% of the  
56 total BVOC emissions globally (Guenther et al., 2006; Helmig et al., 2013; Aydin et  
57 al., 2014) and about 50% in China (Song et al., 2012, Li et al., 2013). In particular,  
58 terrestrial plant foliage is thought to be the major source of atmospheric isoprene  
59 which releases over 90% of isoprene from global forests (Lamb et al., 1987; Guenther  
60 et al., 2006). Extensive investigations have been conducted over the past several  
61 decades to assess BVOC emissions and their potential influences on tropospheric  
62 chemistry and carbon cycle (Lamb et al., 1987; Ceron et al., 2006; Muller et al., 2008;  
63 Chang et al., 2009; Pacifico et al., 2009; Zemankova and Brechler, 2010; Guo et al.,  
64 2013; Calfapietra et al., 2013). Efforts have been also made to measure and simulate  
65 BVOC emissions in China (Wei et al., 2007; Chen et al., 2009; Song et al., 2012; Li et  
66 al., 2013). A recent study by Song et al. (2012) revealed that the annual BVOC  
67 emission in Eastern China was  $11.3 \times 10^6$  t, of which 44.9% was isoprene, followed by  
68 monoterpenes at 31.5%, and other VOCs at 23.6%. The study also showed high  
69 isoprene emissions in boreal forests in Northeastern China, on Qinling – Ta-Pa  
70 Mountains in central China, and in Southern China. Li et al. (2013) estimated the  
71 2003 China's total BVOC emission as 42.5Tg, of which 55% was isoprene emission.

72 BVOC emissions are often thought to be static on decadal or longer time scales  
73 because forest coverage from regional to global scales is assumed to be at steady state

74 (Sanderson et al., 2003; Purves et al., 2004). However, there are concerns for the  
75 potential impacts of climate change and changes in underlying vegetation coverage on  
76 isoprene emissions because leaf level emission intensity depends on biological and  
77 meteorological conditions (Turner et al., 1991; Constable et al., 1999; Ashworth et al.,  
78 2010; Arneth et al., 2008, 2011). Several modeling studies were conducted to assess  
79 the interactions between biogenic isoprene emissions and climate change as well as  
80 the human activities (Constable et al., 1999; Sanderson et al., 2003). Using the USDA  
81 (the United States Department of Agriculture) Forest Service Inventory Analysis  
82 (FIA), Purves et al (2004) estimated decadal changes in BVOC emissions in the  
83 Eastern US between the 1980s and 1990s caused by changes in the extent, structure,  
84 and species composition of forests. They attributed these changes to human-induced  
85 de-forestation and reforestation. Arneth et al. (2008, 2011) compared the responses of  
86 the simulated BVOC emissions derived using different models to climate and  
87 vegetation changes. They found that increasing forest area could add several tens of  
88 percent to future isoprene emissions. Climate change could also exert influences on  
89 isoprene emission via the changes in temperature and CO<sub>2</sub>. The latter can benefit  
90 forest productivity and leaf growth via fertilization effect. Steiner et al (2002)  
91 simulated the effect of human induced land use changes due to urbanization and  
92 agriculture on BVOC emissions. Their results revealed that the increasing  
93 anthropogenic emissions of VOCs subject to urbanization overall enhanced total VOC  
94 emissions. Most of the existing studies were carried out using climate models subject  
95 to projected climate and land cover change scenarios.

96 The Three Northern Regions Shelter Forest (TNRSF) program in China, also  
97 known as ‘the Great Green Wall’, began in 1978 and will terminate in 2050 (**Fig. 1**).  
98 The program aims to increase China’s forest coverage from 5% in the 1970s to 15%  
99 by 2050. By the end of the fourth phase in 2010 of this largest afforestation program  
100 in the human history, the vegetation coverage over the TNRSF has already reached  
101 12.4% (Wang et al., 2011; Central Government of China, 2012). The program has  
102 achieved great successes in mitigating local ecological environment and climate,  
103 despite the debates on the effectiveness of the TNRSF in improving the ecological  
104 environments in Northern China and negative influences of the program on  
105 groundwater storage in arid and semi-arid regions (Pang, 1992; Cheng and Gu, 1992;  
106 Parungo et al., 1994; Hu et al., 2001; Zhong et al., 2001; Ding et al., 2005; Liu et al.,  
107 2008; Yan et al., 2011; Zheng and Zhu, 2013; Fang et al., 2001; Tan et al., 2007;  
108 Zhang et al., 2013). Recently, the TNRSF impact on air quality was also investigated  
109 (Zhang et al., 2015), which showed that the increased vegetation coverage in the  
110 TNRSF has increased its efficiency in removing air contaminants from the  
111 atmosphere as supported by the increased modeled dry deposition velocities and  
112 fluxes of sulfur dioxide (SO<sub>2</sub>) and NO<sub>x</sub> in many places of the region during the past  
113 three decades.

114 Given its unique status in large-scale artificial afforestation in the human history,  
115 the TNRSF might provide significant insights into understanding of human induced  
116 biogenic VOC emissions on a long-term scale. In the present study, a framework  
117 combining satellite remote sensing data, a biogenic emission model, and uncertainty

118 analysis was first developed to estimate BVOC emissions in Northern China.  
119 Seasonal and annual biogenic isoprene emission inventories were then developed  
120 from 1982 to 2010. Finally, the potential influences of the development and expansion  
121 of the TNRSF on the long-term trends of the biogenic isoprene emissions were  
122 investigated to discern evidence of decadal or longer-term changes in BVOC  
123 emissions from large-scale forest restorations induced by the human activities. The  
124 newly generated historical isoprene emissions inventories over Northern China will  
125 also be useful for assessing past, current, and future air quality and climate issues.

126

## 127 **2. Methodology**

### 128 **2.1. BVOC emission model**

129 The MEGAN2.1 (Model of Emissions of Gases and Aerosols from Nature version 2.1)  
130 (Guenther et al., 2012) which is an updated version of MEGAN2.0 (Guenther et al.,  
131 2006) and MEGAN2.02 (Sakulyanontvittaya et al., 2008), was used here to estimate  
132 BVOC emissions in Northern China. This new version includes additional compounds,  
133 emission types, and various controlling processes. For BVOC emissions, MEGAN2.1  
134 is primarily driven by biological and meteorological factors, including vegetation type  
135 with which the emission factors of BVOCs are assigned, air and leaf temperatures,  
136 light, leaf age and leaf area index (LAI), solar radiation/photosynthetically active  
137 radiation (PAR), wind speed, humidity, and soil moisture (Guenther et al., 2006; 2012;  
138 Pfister et al., 2008; Arneth et al., 2011). MEGAN2.1 was set up over Northern China  
139 with a grid spacing of  $0.25^\circ \times 0.25^\circ$  latitude/longitude to produce gridded daily and  
140 monthly emission fluxes. Meteorological data used in the MEGAN2.1 employed the

141 6-hourly objectively analyzed data from the  $1^{\circ}\times 1^{\circ}$  latitude/longitude NCEP (National  
142 Centers for Environmental Prediction) Final Operational Global Analysis  
143 (<http://dss.ucar.edu/datasets/ds083.2/>). These data were then interpolated into the  
144 TNRSF grids on the spatial resolution of  $0.25\times 0.25$  latitude/longitude. PAR was  
145 calculated from solar radiation provided by the Big-leaf dry deposition model (Zhang  
146 et al., 2002). Twenty-two land types were used, including an additional crop type  
147 which was not specified in the MEGAN2.1. These land types at each model grid were  
148 identified using the surface roughness lengths estimated from satellite remote sensing  
149 data (Zhang et al., 2015). Guenther et al. (2012) reported the differences in  
150 MEGAN2.1 modeled annual isoprene emissions as a result of changing plant  
151 functional type (PFT) (24 %), LAI (29 %), and meteorology (15 %) input data. This  
152 suggests that LAI is one of crucial variables in the model.

153 To evaluate the MEGAN2.1 estimated isoprene biogenic emission fluxes, a field  
154 campaign was conducted to measure total VOC (TVOC) concentrations at several  
155 sites within and outside the TNRSF (Section 2.4). The monitored TVOC  
156 concentrations were then converted to TVOC emission fluxes using a box model,  
157 developed by Guenther et al (1996) which links biogenic VOC emission and  
158 photochemical reaction with OH radicals and ozone. The model was derived from a  
159 simplified mixed-layer scalar conservation equation, given by

$$160 \quad E = z_i L c, \quad (1)$$

161 where  $E$  and  $c$  are the emission and concentration in the mixed-layer,  $z_i$  is the height  
162 of mixed-layer capping inversion, taken as 1000 m following Guenther et al (1996).  $L$

163 is the oxidation rate of VOC subject to OH radical and ozone, defined as  $[k_{\text{OH}}, \text{OH}] +$   
164  $[k_{\text{O}_3}, \text{O}_3]$ , where  $k_{\text{OH}}$  and  $k_{\text{O}_3}$  are reaction rate constants for OH and O<sub>3</sub>, respectively.  
165 The rate constants and mean concentrations of OH and ozone are presented in Table  
166 S1 of Supplementary Materials. Further details are presented in Sections 2.4 and 3.4.

## 167 **2.2. LAI.**

168 LAI data with 0.25°×0.25° latitude/longitude resolution from 1982 to 2010 were  
169 derived from the satellite remote sensing data of the normalized difference vegetation  
170 index (NDVI) for the same period. Detailed descriptions of the procedures generating  
171 LAI data for the TNRSF region were presented in Zhang et al (2015).

## 172 **2.3. Uncertainty analysis.**

173 Although the BVOC emissions model was well established for different vegetation  
174 types, there were uncertainties in the estimate of BVOC emission fluxes. Some of  
175 these uncertainties are generated from inaccurate emission factors, empirical  
176 algorithms, and input data used in the model (Hanna et al., 2005; Guenther et al.,  
177 2012). Situ et al showed that, in addition to the emission factors, PAR and  
178 temperature also created large uncertainties in the MEGAN model (Situ, et al., 2014).  
179 A Monte Carlo technique was used to evaluate uncertainties of modeled isoprene  
180 emissions by MEGAN2.1 (Hanna et al., 2005; Guenther et al., 2006, 2012; Situ et al.,  
181 2014). In the uncertainty analysis, each input parameter in MEGAN2.1 for isoprene  
182 emissions, including LAI, leaf temperature (a function of air temperature), PAR,  
183 emission factors, several empirical coefficients related to past leaf temperatures, and  
184 solar zenith, was treated as a random variable with a normal distribution. The



185 MEGAN2.1 model for BVOC emissions was run repeatedly 100,000 times at the 95%  
186 confidence level based on the coefficients of variation (*CV*, %) of these input  
187 parameters. The Monte Carlo simulations showed that the isoprene emissions reached  
188 approximately a normal distribution, ranging from 0.05 to 5.29 micro-mole m<sup>-2</sup> h<sup>-1</sup>  
189 with the variation from 97%-211%. Details for the uncertainty analysis are presented  
190 in Supplementary Materials (Table S2, **Fig. S1**).

191 The uncertainty analysis using the Monte Carlo technique was also conducted for  
192 the box model (Eq. 1). Analogous to the uncertainty analysis for the MEGAN2.1, this  
193 box model was also run repeatedly 100,000 times at the 95% confidence level based  
194 on the coefficients of variation (*CV*, %) for  $z_i$ , the measured isoprene concentration  
195 (*C*), and the concentrations of OH and O<sub>3</sub>. The *CV* for these four parameters were  
196 taken from Guenther et al (1996) (Table S3). The results from Monte Carlo  
197 simulations showed that the converted isoprene emissions from the measured  
198 concentrations using Eq. 1 reached approximately a normal distribution, ranging from  
199 1.2 to 152.9 μg m<sup>-2</sup> h<sup>-1</sup> with the variation from 98.3%-116.7% (**Fig. S2**).

#### 200 **2.4. Ambient VOCs concentrations within and outside the TNRSF.**

201 As part of efforts to understand potential uncertainties in the estimation of isoprene  
202 emissions from the TNRSF, a field campaign was conducted to measure gas-phase air  
203 pollutants, particular matter, and persistent organic pollutants in air, foliage, and soil  
204 within and outside the TNRSF in the summer of 2015. The first phase of this field  
205 study focused on the Central-North China region of the TNRSF because this region  
206 has been paid the highest attention by the TNRSF program due to its proximity to

207 Beijing and Tianjin, the two megacities in Northern China. Eight monitoring sites in  
208 this region were selected, with four of these inside and another four outside the forest  
209 (**Fig. S3**). All these sites are situated in the northwest and northeast of Beijing where  
210 the TNRSF program was operated most successfully. Total VOC (TVOC) was  
211 measured simultaneously using the GreyWolf TG-502/TG-503 sensors (GreyWolf  
212 Sensing Solutions) at each paired sites within and outside the forest but on different  
213 days at the selected 4 paired sites. The sampling frequency was set at 1 min. The  
214 GreyWolf TG-502/TG-503 instrument uses SEN-B-VOC-PPB PID (photoionization  
215 detector) sensor (10.6eV lamp, range: 5 to 20,000 ppb) which responds to the vast  
216 majority of VOCs with the response time < 1 min. The environmental conditions for  
217 sensor operating range from 0 to 90% RH (relative humidity) and from -15° to 60° C.  
218 The GreyWolf TVOC sensor adopts two points calibration approach with low point of  
219 0 ppb and high point at 7500~9000 ppb, respectively. Standard calibration gas is  
220 isobutylene. More details of the GreyWolf TG-502/TG-503 TVOC sensor can be  
221 found at the GreyWolf website ([https://www.wolfsense.com/directsense-tvoc-volatile-](https://www.wolfsense.com/directsense-tvoc-volatile-organic-compound-meter.html)  
222 [organic-compound-meter.html](https://www.wolfsense.com/directsense-tvoc-volatile-organic-compound-meter.html)). It should be noted that the GreyWolf VOC sensor can  
223 only measure TVOC, hence the concentration of individual VOC species is not  
224 reported here. Typical tree species planted in this region were selected in the field  
225 monitoring program. Among them, poplars (*Populus spp*), a broadleaf tree species,  
226 dominated the two forest sites in Langfang and northern Zhangbei County. Poplars  
227 has been the major tree species planted across the Central-North China region of the  
228 TNRSF over the last thirty years. From the late half of the 2000s, due to the death of

229 many poplars in this region, Scots pine (*Pinus sylvestris*), which is a coniferous tree  
230 species, has been recommended and planted in this region. Scots pine is the major tree  
231 species at northern Zhangbei County and Xinglong forest sites. As for the  
232 comparative monitoring sites outside the forests, the Langfang site is 500 m away  
233 from the forest and located in a corn field, the Zhangbei north and south sites are  
234 about 1 km and 600 m, respectively, away from the forest and both are located in a  
235 grassland, and the Xinglong site is about 400 m away from the forest and located in a  
236 corn field. The sampling was operated in early morning from 6:15 – 8:15am, and  
237 early afternoon from 2:15 – 4:15 pm with sampling frequency of 1 min. The sampling  
238 date was on August 9<sup>th</sup>, 2015 at the Langfang sites, 10<sup>th</sup> at the Xinglong sites, 12<sup>th</sup> at  
239 the Zhangbei north sites, and 13<sup>th</sup> at the Zhangbei south sites. It should be noted that  
240 this field measurement program was not aimed to determine the spatial and temporal  
241 distributions of isoprene emissions, but instead to examine and verify the release of  
242 this reactive biogenic VOC species from the TNRSF.

### 243 **3. Results**

#### 244 **3.1. Isoprene emission inventory in TNRSF**

245 **Figure 2** shows the TNRSF domain-averaged annual biogenic isoprene emissions  
246 (micro-moles m<sup>-2</sup> h<sup>-1</sup>) aggregated from monthly values. The magnitudes of isoprene  
247 emissions estimated in the present study agree with the China's BVOC emission  
248 inventory established previously, particularly in the natural forests (Song et al., 2012;  
249 Li et al., 2013), as elaborated below. A long-term increasing trend up to 2007,  
250 although with fluctuations in certain years, was observed (**Fig . 2**) The Central-North

251 region of the TNRSF exhibited the strongest increasing trend with the highest  
252 emissions increase by 58% over the 30 years period.

253 **Figure S4** illustrates the MEGAN2.1 simulated isoprene emission fluxes across  
254 the TNRSF in 1982, the early stage of the TNRSF construction, and 2010, the end of  
255 the fourth phase (2001-2010) of the program, respectively. Compared with the  
256 emission fluxes in 1982, higher isoprene emissions in the Central-North China region  
257 and lower emission fluxes in the Northeast region and Eastern Inner Mongolia region  
258 of the TNRSF were identified in 2010. The differences in the biogenic isoprene  
259 emissions between 1982 and 2010 were calculated as  $E_{dif} = E_{2010} - E_{1982}$ . The spatial  
260 pattern of  $E_{dif}$  (**Fig. 3**) is consistent with the emission fluxes in 1982 and 2010, as  
261 shown in **Fig. S4a** and **b**. Positive differences of  $E_{dif}$  were observed in the  
262 mountainous areas of west Xinjiang, Shaanxi, eastern Gansu provinces, and the  
263 Central-North China region, suggesting increasing isoprene emissions associated with  
264 the expansion of the TNRSF in these regions.

### 265 **3.2. Isoprene emission trend in the TNRSF and Northern China**

266 Decadal or longer time trends in isoprene emissions over the TNRSF and Northern  
267 China can provide some insights into the impact of the large-scale artificial  
268 afforestation on BVOC emissions - the knowledge that is needed to address air quality,  
269 climate, and ecosystem issues. **Figure 4** illustrates modeled isoprene emission fluxes  
270 (micro-moles  $\text{m}^{-2} \text{hr}^{-1}$ ) in 2000 (**Fig. 4a**), after 20 years construction of the TNRSF,  
271 and the slopes (trends) of the linear regression relationship between isoprene emission  
272 and the time sequence of 1982 through 2010 (**Fig. 4b**) over Northern China,

273 respectively. High isoprene emissions can be found in the regions extending from  
274 northeast Qinghai province to Ta-Pa Mountains, the boreal forest in Northeast China,  
275 Central-North China, and Tianshan Mountain and Pamirs in Xinjiang province. The  
276 spatial pattern of the estimated emissions in Northeastern China is similar to Song et  
277 al.'s results from 2008 to 2010 (Song et al., 2012). They showed high isoprene  
278 emissions from the boreal forest in Northeastern China and Qinling – Ta Pa  
279 Mountains.

280 The total annual isoprene emission, summed from annual emissions of the model  
281 grids that fall within the TNRSF domain, ranged from 45,000 to 70,000 ton yr<sup>-1</sup>  
282 during 1982-2010 for the whole TNRSF (the area encircled by the blue solid line in  
283 **Fig. 4**), and from 132,000 to 176,000 ton yr<sup>-1</sup> for whole Northern China (**Fig. 4**). This  
284 is equivalent to a total emission of 1.6 Tg and 4.4 Tg, respectively, for the two regions  
285 during the past three decades from 1982 to 2010. It is worth noting that, although the  
286 TNRSF accounts for 59% of the total area of Northern China and 42% of mainland  
287 China (Zhang, et al., 2015), it covers almost all arid and semi-arid regions in Northern  
288 China. Vegetation coverage in these regions was still sparse after 30 years  
289 construction of the TNRSF, and shrubs, instead of trees, are major plant types in the  
290 Western China region of the TNRSF. The isoprene emissions are considerably low in  
291 these regions, as shown by **Figs. 4** and **5**. In addition, as shown by **Fig. 4**, the region  
292 of Northern China defined in this study extends virtually to 30°N. Although the  
293 isoprene emissions in the TNRSF only accounted for 37% of the total emissions in  
294 Northern China, the relatively strong increasing trend (**Fig. 2**) in the TNRSF

295 (slope=0.881,  $R^2=0.335$ ) has reversed the negative trend (slope=-0.533,  $R^2=0.05$ ) of  
296 the total annual isoprene emissions in Northern China, which did not take the isoprene  
297 emissions in the TNRSF into consideration, to the positive trend (slope=0.347,  
298  $R^2=0.014$ ) from 1982 to 2010 in Northern China, as shown in **Fig. S5**.

299 To highlight the contribution of the TNRSF to the increasing isoprene emissions,  
300 the trend of the gridded isoprene emissions over the TNRSF was further investigated.  
301 As expected, the estimated monthly emission fluxes showed dramatic seasonal  
302 variations with the largest values in summer and the lowest values in winter,  
303 consistent with the seasonal changes in LAI over the TNRSF (figure not shown).  
304 **Figure 5** presents the gridded trends of the summer biogenic isoprene emissions (Eq.  
305 1) across the TNRSF from 1982 to 2010. The summer emission fluxes exhibit similar  
306 annual pattern to the annual emissions (**Fig. 4b**) but are greater than the annual  
307 emissions, as shown by **Fig. 5**. Positive trends of the emissions were observed in the  
308 mountainous and surrounding areas of the Junggar Basins (north Xinjiang), eastern  
309 Qinghai province in the Northwest China region of the TNRSF, the Central-North  
310 China region, and western Liaoning province in the Northeast China region of the  
311 TNRSF. These provinces and locations are marked in **Fig. 1**. In particular, the largest  
312 positive trends can be observed in the areas north of the two megacities - Beijing and  
313 Tianjin. These two megacities have been targeted as key cities to be protected by the  
314 TNRSF from sandstorms from the north. Extensive tree planting activities have been  
315 promoted to the north of these two megacities (Central Government of China, 2012).

316 **Figure 6** shows the isoprene emissions from 1982 to 2010 averaged over the

317 Northwest China, the Central-North China, and the Northeast China regions of the  
318 TNRSF, respectively. It can be identified again that the domain averaged isoprene  
319 emissions in the Central-North China region of the TNRSF exhibited a clear  
320 increasing trend with the slope of 0.0004 ( $R^2 = 0.35$ ,  $p=0.002$ ). Whereas, statistically  
321 insignificant and relatively weak trends of isoprene emissions were found in the  
322 Northeastern China (slope=0.00003,  $R^2=0.032$ ,  $p=0.484$ ) and Northwestern China  
323 (slope=0.00009,  $R^2=0.27$ ,  $p=0.012$ ) regions of the TNRSF, respectively. The increase  
324 of isoprene emissions over the Central-North China region can be attributed to  
325 continuous expansion of forest coverage. Compared with the Central-North region of  
326 the TNRSF, the forests in the Northeast China region are mixed with natural forests.  
327 These natural forests already reached the steady state before the 1980s, so they would  
328 not contribute to the increasing trend of biogenic isoprene emissions. As shown by  
329 **Fig. 4b**, the isoprene emissions in most places of Northeast China show almost no  
330 trends in most places of Northeast China. The Northwest China region of the TNRSF  
331 is arid and semi-arid area with low precipitation. Shrubs, instead of trees, were  
332 planted in many places of this part of the TNRSF regions, resulting in low biogenic  
333 isoprene emissions.

334 Trends of isoprene emissions were also compared between those within and  
335 outside the TNRSF and in natural forests. Three small areas were selected for the  
336 comparison, each consisting of 4 grid points, in the Central-North China region of the  
337 TNRSF (marked by the red circle in the inner map of **Fig. 1**), a farmland outside the  
338 TNRSF (blue circle), and in the boreal forest of Northeast China (the Greater Khingan

339 Mountains, marked by yellow circle in **Fig. 1**), respectively. Trends in annually  
340 averaged isoprene emissions from these three small areas are shown in **Fig. 7**.  
341 Significant increasing trend is only seen in the area within the TNRSF. The levels of  
342 isoprene emissions in the other two small areas were almost uniformly distributed for  
343 the last three decades.

### 344 **3.3. Comparison with the previous emission data**

345 No extensive and direct measurements of BVOC emission across the TNRSF have  
346 been ever carried out. Several field campaigns were conducted to measure BVOC  
347 emissions in Northern China but these monitoring programs were not typically  
348 designated for the TNRSF (Klinger et al., 2002; Wang et al., 2003). Li et al. (2013)  
349 established an emission inventory of BVOCs (isoprene, monoterpenes, sesquiterpene  
350 and other VOCs) over China using MEGAN2.1 model. Their results showed that  
351 annually averaged isoprene emission fluxes ranged from 0 to  $22 \mu\text{g m}^{-2} \text{h}^{-1}$  in 2003 in  
352 northern Xinjiang, Qinghai, Gansu, and Shaanxi provinces in the Northwest China  
353 region of the TNRSF, and western Inner Mongolia. The average isoprene emission  
354 fluxes estimated in the present study for the same regions and the same year ranged  
355 from  $0.01$  to  $18.2 \mu\text{g m}^{-2} \text{h}^{-1}$ , agreeing reasonably well with Li et al's  
356 inventory (2013) also showed high isoprene emission flux in the Central-North China  
357 region, including the north of Shanxi and Hebei provinces, Beijing, and the natural  
358 (boreal) forest area in Northeast China, ranging from  $22$  to  $880 \mu\text{g m}^{-2} \text{h}^{-1}$ . While the  
359 lower limit of their estimated flux agrees well with our lowest emission flux of  $20.4$   
360  $\mu\text{g m}^{-2} \text{h}^{-1}$ , the upper limit of their emission flux was  $880 \mu\text{g m}^{-2} \text{h}^{-1}$ , a factor of 4



361 higher than our value ( $122.4 \mu\text{g m}^{-2} \text{h}^{-1}$ ) for the same region. Li et al (2013) adopted  
362 more locally updated species-specific emission factors and a vegetation classification  
363 based on a new vegetation investigation in the late 1990s and early 2000s in China.  
364 Their calculation also used hourly and diurnal meteorological (temperature, radiation,  
365 winds) data. Our estimated fluxes used the emission factors specified in the  
366 MEGAN2.1 (Guenther et al., 2012) and vegetation types classified by the roughness  
367 lengths (Zhang et al., 2002, 2015). In addition, our model input daily meteorological  
368 data. These different input data to the MEGAN model resulted likely in the difference  
369 of the isoprene emission fluxes between Li et al (2013) and our results. Song et al.  
370 (2012) simulated BVOC emissions in Eastern China from 2008 to 2010. A portion of  
371 their model domain in Eastern China superimposed with the Central-North China and  
372 the Northeast China region of the TNRSF defined in our study. The annually averaged  
373 isoprene emission fluxes from 2008 to 2010 from Song et al's model simulations  
374 ranged from 10 to  $100 \mu\text{g m}^{-2} \text{h}^{-1}$  in Inner Mongolia region, and  $100\text{-}1000 \text{g m}^{-2} \text{h}^{-1}$  in  
375 the north of Shanxi and Hebei provinces, Beijing, and Tianjin, which were higher than  
376 our results of 0 to  $32.6 \mu\text{g m}^{-2} \text{h}^{-1}$  and 20.4 to  $122.4 \mu\text{g m}^{-2} \text{h}^{-1}$ , respectively, in these  
377 two regions. Song et al. used MEGAN2.04 model with different emission factors  
378 adjusted based on China's principal vegetation species (Song et al., 2012). These  
379 could also lead to different biogenic isoprene emissions.

#### 380 **3.4. Emissions converted from ambient concentrations**

381 **Figure 8** illustrates measured afternoon (local time 2-4 pm) TVOC levels in the  
382 atmosphere at the 4 paired monitoring sites in the Central-North China region of the

383 TNRSF with sampling frequency of 1 min. Detailed descriptions of these sites and  
384 sampling procedures are presented in Methodology section, **Fig. S3**, and Table S4,  
385 respectively. Higher TVOC air concentrations were observed at all forest sites than  
386 those sites outside the forests. In particular, the TVOC levels at the southern and  
387 northern Zhangbei sites within the TNRSF were 3 to 4 times higher than that  
388 measured in the grassland sites outside the TNRSF, suggesting that the forests made  
389 significant contributions to the sampled TVOC levels. Using the box model (Eq. 1),  
390 emission fluxes were converted from the measured TVOC concentrations at the four  
391 forest sites. Taking the TVOC levels as the box model input (Eq. 1), and assuming  
392 the isoprene emission to be 50% of the TVOC (Song et al., 2012; Li et al., 2013), we  
393 obtained the emission fluxes of 32.3, 44.1, 52.9, and 44.1  $\mu\text{g m}^{-2} \text{h}^{-1}$  at the Langfang,  
394 Xinglong, Zhangbei (North), and Zhangbei (South) sites, respectively. These values  
395 agree nicely with the MEGAN2.1 modeled emission fluxes of 36, 41.5, 49, and 47.6  
396  $\mu\text{g m}^{-2} \text{h}^{-1}$  at the same sites. It is noticed that the box model (Eq. 1) does not take into  
397 account the effect of wind speed on the emissions. An effort was also made to use a  
398 simplified Gaussian model (Eq. S1) for an area source (Arya, 1999) to convert the  
399 measured TVOC concentrations to emissions. Under approximately calm wind  
400 conditions ( $<0.5 \text{ m s}^{-1}$ ) at the sampling sites and the same assumption of isoprene  
401 emission as the half of the TVOC emission, the converted fluxes using this model are  
402 about a factor of 2 higher than the MEGAN2.1 estimated fluxes. Results are presented  
403 in Supplementary Materials. The potential differences between the MEGAN2.1  
404 modeled and converted fluxes from the Gaussian model (Eq. S1 of Supplementary)

405 might be attributed to several causes. Firstly, the TVOC concentrations were  
406 measured at a single site within the selected forests in this field campaign which  
407 represent typical tree species in the Central-North China region of the TNRSF.  
408 Whereas, the underlying surface of a model grid square ( $27.83 \times 27.83 \text{ km}^2$ ) is not  
409 fully covered by trees but consists of other surface types, such as croplands, bare soils,  
410 water surfaces, and towns where BVOC emissions might be lower. In addition, in the  
411 simplified Gaussian model (Eq. S1, Supplementary) we choose the fetch  $\Delta l = 3\text{km}$   
412 which is related directly to the magnitude of the converted emission fluxes which was  
413 subject to uncertainties. Nevertheless, overall the converted fluxes from the measured  
414 TVOC concentrations using the simplified Gaussian model are about the 2 fold of the  
415 modeled fluxes, suggesting the reasonable accuracy of the MEGAN model applied in  
416 the present investigation.

417 It is worthwhile to note that anthropogenic VOC might contribute to the ambient  
418 concentrations of TVOCs measured at these selected sampling sites. In addition, the  
419 emissions and concentration ratios are not identical for all VOCs due to their  
420 different reactivity. A VOC can be emitted in relatively low amounts but make a large  
421 contribution to the TVOC if it is considerably less reactive than isoprene. Wang et al  
422 (2014) collected ambient concentrations of VOCs at 27 sites across Beijing from July  
423 2009 to January 2012, including urban, suburban, and rural sites. To identify  
424 potential sources of isoprene, they estimated the ratio of isoprene to 1,3-butadiene.  
425 While the reactivity for these two VOC compounds was similar, their emission  
426 sources differ significantly. Vehicular exhaust was found to be the dominant source of

427 1,3-butadiene in Beijing (Wang et al, 2010) whereas isoprene was largely related to  
428 biogenic emissions. Their results showed that the wintertime isoprene/1,3-butadiene  
429 was 0.30–0.34 ppbv ppbv<sup>-1</sup>, characterizing the emission from vehicular exhaust in  
430 Beijing (Wang et al. 2010), suggesting that the atmospheric isoprene during the  
431 wintertime was emitted mostly from vehicular exhaust In the warm period (May -  
432 September), their measured ratios of isoprene/1,3-butadiene ranged from 16 to 43  
433 ppbv ppbv<sup>-1</sup>, two order of magnitude higher than that in the wintertime, indicating that  
434 the summertime isoprene was released from biogenic sources. Considering that our  
435 sampling sites (especially the Langfang and Xinglong sites) are close to Beijing and  
436 covered by similar tree species to those planted in the suburban and rural areas of  
437 Beijing, the results from Wang et al (2014) might be applicable in our cases because  
438 our measurements were also taken in the summertime (August). In particular, our  
439 sampling sites are all located in rural areas, far away from traffic, industrial, and  
440 residential areas, indicating weak influence of the anthropogenic emissions on the  
441 measured TVOC level, half of which has been hypothesized to be isoprene in the  
442 present study.

#### 443 **4. Discussions**

444 Overall the estimated biogenic isoprene emission fluxes across the TNRSF illustrated  
445 an increasing trend from the 1980s onward (**Fig. 2**). The incline trend was most  
446 significant in the Central-North region of the TNRSF where most intensive  
447 afforestation has been carried out in Northern China (Zhang and Zhu, 2013), in order  
448 to protect the national capital (Beijing) region from dust and sandstorms. The

449 increasing biogenic isoprene emissions can be attributed to the development of the  
450 TNRSF. The forest expansion in the TNRSF can be identified by the satellite derived  
451 LAI, as seen from **Fig. S6a** and **b**. The linear increasing trend of the LAI across the  
452 TNRSF is consistent with the modeled isoprene emission fluxes. The maximum  
453 increase (58%) of the isoprene emissions from 1982 to 2010 in the Central-North  
454 region of the TNRSF seems to agree well with the model prediction by Arneth et al.  
455 (2008, 2011) based on projected land use changes. Their modeling results suggested  
456 that increasing forest area could lead to several tens of percent change in biogenic  
457 isoprene emissions.

458 As shown above, the significant incline trend of the annual total isoprene  
459 emissions in the TNRSF has affected the long-term trend of the emission in Northern  
460 China. This implies that the increasing emission trend across the TNRSF could alter  
461 the large-scale BVOC emissions not only in the TNRSF, but also in Northern China.  
462 Considering that the TNRSF occupies 59% of Northern China and 42% of whole  
463 mainland China. Future impacts of the TNRSF on BVOC emissions may be even  
464 stronger with continuous increase of vegetation coverage till the end of the program  
465 in 2050.

466 While BVOC emissions vary on short time scales, the global BVOC emissions  
467 are often assumed to change little on long-term (e.g., decadal) scale (Purves et al.,  
468 2004; Sindelarova et al., 2014) considering the steady state of global forests. Since  
469 BVOCs can partition onto or form particles in the atmosphere after oxidation, their  
470 emissions could affect aerosol formation, cloud condensation nuclei, and climate

471 (Makkonen et al., 2012, Penuelas and Staudt, 2010). Identification of the impact of  
472 climate change on BVOC emissions is not straightforward if regional or global  
473 forests reach a steady state. The evidence identified in this study suggested that the  
474 human-induced BVOC emissions via large-scale afforestation exert strong influence  
475 on long-term BVOC emission and should be taken into consideration in projected  
476 climate change scenarios, at least on a regional scale, such as Northern China. As a  
477 precursor of secondary organic aerosols and tropospheric ozone, the significant  
478 incline of biogenic isoprene emissions also carry significant implications to the air  
479 quality in Northern China. Heavy air pollutions in Beijing-Tianjin-Hebei (**Fig. 1**) have  
480 been widely known nationally and internationally, characterized by year round high  
481 levels of fine particular matter (PM<sub>2.5</sub>) and high surface ozone concentrations in the  
482 summertime. Chinese government has decided to extend the TNRSF as one of the  
483 primary measures to reduce and remove air pollutants from Beijing-Tianjin-Hebei  
484 area (Chinese Environmental Protection Agency, 2013). As shown in **Figs. 5** and **6**,  
485 the TNRSF in the Central-North region covering a large part of Beijing-Tianjin-Hebei  
486 area has already gained the most rapid development as compared to the other two  
487 northern regions of the TNRSF (**Fig. 1**), leading to marked incline of isoprene  
488 emissions. However, it is not yet clear if and how the extension of the TNRSF could  
489 otherwise improve local air quality. Our previous study suggested that the TNRSF  
490 played a moderate role in removing SO<sub>2</sub> and NO<sub>x</sub> (Zhang et al., 2015). Under the  
491 rapidly increasing NO<sub>x</sub> emissions in the past decade due to rapidly increasing number  
492 of private vehicles in Beijing-Tianjin-Hebei area, it is necessary to assess the

493 interactions between BVOC emissions from the TNRSF and local air quality in this  
494 region.

495 In addition to its long-term trend, isoprene emission also exhibited short-term  
496 interannual fluctuations, as also observed from **Fig. 2**. Factors causing the fluctuations  
497 or interannual changes in the emission fluxes depend on meteorological and  
498 biological processes. Afforestation and deforestation often took place during the  
499 course of the TNRSF construction due to favorable or unfavorable weather and  
500 climate conditions for tree growth. For example, 10% - 50% of trees planted since the  
501 late 1970s in the Central-North region of the TNRSF were reported dead since 2007  
502 (Zhang et al., 2013; Tan and Li, 2015), causing visible decline of the forest coverage  
503 and isoprene emissions in this region after 2007, as shown in **Fig. 2**. The lower  
504 isoprene emission in 2010 in the Northeast China region and eastern Inner Mongolia  
505 region of the TNRSF as compared with that in 1982 was inconsistent with the  
506 increasing trend of the emission. The forest coverage in the Northeast China region  
507 did not show considerable change between 1982 and 2010. On the other hand, lower  
508 annual temperatures (e.g., by around 1°C) in 2010 than in 1982 were evident over the  
509 Northeast China region of the TNRSF (**Fig. S7a**), which likely caused lower biogenic  
510 emissions in 2010 (Purvis et al., 2004; Arneth et al., 2008, 2011). In addition,  
511 compared with the increasing trend of LAI in the Northeastern China region of the  
512 TNRSF (**Fig. S6a**), no statistically significant increasing trends of the isoprene  
513 emissions are discerned in this region. **Figure S7b** displays the trend of annual  
514 surface air temperatures (SAT, °C) in the Northeast China region of the TNRSF from

515 1982 to 2010. Overall the SATs exhibited a decreasing trend, caused mostly by  
516 declining SATs since the late 1990s. Since temperature plays a key role in canopy  
517 BVOC emissions (Guenther et al., 2012; Li et al., 2013), the lack of the incline trend  
518 of the isoprene emission fluxes in the Northeastern China region of the TNRSF might  
519 be attributable to the decreasing SAT from the late 1990s. Another environmental  
520 factor that may exert the influence on the trend of isoprene emissions is solar  
521 radiation/PAR (Situ et al., 2014). Analogous to the response of the BVOC emissions  
522 to temperature, increasing radiation could also enhance the isoprene emissions, or  
523 vice versa, particularly on daily or monthly basis.

524         The comparison between the isoprene emission trends and the emissions in  
525 2000 in Northern China also carries a significant implication for the human induced  
526 BVOC emissions. As shown from **Fig. 4b**, the trend of isoprene emissions from 1982  
527 to 2010 over Northern China showed a rather different spatial pattern from its  
528 emissions in 2000 (**Fig. 4a**). No significant trends were observed in the boreal forest  
529 in Northeastern China, though a larger amount of isoprene was emitted from the  
530 forest in this region in 2000. This implies that this natural forest was likely under a  
531 steady state from which the biogenic isoprene emissions were not altered on the  
532 decadal basis (Sanderson et al., 2003; Purves et al., 2004).

533         Although Qinghai – Ta-Pa Mountains exhibited the highest emissions in 2000  
534 (**Fig. 4a**), negative trends of the biogenic isoprene emissions dominated this area,  
535 indicating the declining of the emissions over the period of 1982 through 2010. This  
536 is consistent with the decreasing vegetation coverage during this period in this region,



537 as shown by the negative trends of the leaf area index (LAI) in Northern China (**Fig.**  
538 **S6**). On the other hand, most positive trends can be identified in the Central-North  
539 region and along the foots of Tianshan Mountain in west China (see the areas  
540 encircled by the solid blue line in **Fig. 4**). This manifests that the TNRSF exerts strong  
541 influences on biogenic VOC emissions, particularly on their decadal variation, though  
542 the magnitude of emissions might not be higher than that from natural forests in  
543 Northeastern China (**Fig. 4a**). Results further imply that the TNRSF is very likely the  
544 major source contributing to the increasing biogenic isoprene emissions over the past  
545 30 years and many years to come in Northern China. Climate change has been  
546 thought also to play an important role in the changes in biogenic emission of isoprene  
547 on decadal or longer time scale because it can alter temperature and vegetation  
548 coverage (Turner et al., 1991; Sanderson et al., 2003). It is unknown if and to what  
549 extent the increasing vegetation coverage and temperature over the TNRSF were  
550 induced by climate change. Evidence shows that the human induced afforestation  
551 contributed mostly to the increased vegetation coverage over the TNRSF and  
552 Northern China (Wang et al., 2011), as shown by **Fig. S6a**, and hence to the increased  
553 biogenic isoprene emissions

554 Among the three small areas within the TNRSF, in the farmland, and in the  
555 boreal forest of Northeastern China (**Fig. 7**), the emission values increased by nearly 5  
556 times from 1982 to 2010 in the area within the TNRSF with the slope of 0.0018 ( $R^2 =$   
557 0.55). On the other hand, no statistically significant increasing trends of biogenic  
558 isoprene emissions were found in the farmland and the boreal forest, though the

559 higher emissions were observed in the boreal forest. More interestingly, the biogenic  
560 isoprene emissions in the selected small area of the Central-North China region tend  
561 to surpass the isoprene emissions in the boreal forest from 2004 onward. This can be  
562 partly attributed to rapidly growing forest coverage and higher temperatures in this  
563 region as compared to Northeastern China. The large area of foliage trees planted in  
564 this region also played a role for relatively high and increasing isoprene emissions as  
565 compared with the boreal forests in Northeast China where coniferous trees are major  
566 tree species which release relatively lower isoprene to the atmosphere as compared to  
567 broadleaf trees in the selected area in the Central-North China region of the TNRSF  
568 (Guenther et al, 2012).

## 569 **5. Conclusions**

570 Gridded monthly and annual biogenic isoprene emissions in Northern China were  
571 modeled for the period of 1982 to 2010 and were then applied to assess the long-term  
572 trends of the biogenic isoprene emissions in the TNRSF in order to discriminate the  
573 signals of the human activities in decadal and longer-term trends of BVOCs on large  
574 spatial scales. Significant impacts of the TNRSF on the BVOC emissions in Northern  
575 China were identified during the past three decades. Annual isoprene emissions in  
576 many places of the TNRSF region, especially in the Central-North China region,  
577 exhibited an inclining trend. The maximum increase in the isoprene emission flux  
578 reached 58% between 1982 and 2010, indicating important roles of the human  
579 activities on BVOC emissions. The comparison of isoprene emission fluxes among  
580 the Central-North China region of the TNRSF, farmland, and the boreal forest in

581 Northeastern China outside the TNRSF revealed that the biogenic isoprene emissions  
582 in some areas of the Central-North China region of the TNRSF produced by man-  
583 made forests have surpassed the emissions from the natural forests. This suggests that  
584 the TNRSF was a main contributor to the decadal or longer-term changes in BVOCs  
585 in Northern China. The impact of the TNRSF on BVOC emissions is expected to be  
586 stronger in the coming years along with continuous development of the TNRSF  
587 program till 2050. Since VOCs are major precursor of tropospheric ozone, future  
588 studies are needed to investigate how the increased BVOCs in the TNRSF contribute  
589 to ozone formation, especially in the case of concurrently increasing NO<sub>x</sub> emissions in  
590 Northern China.

591 **The Supplement related to this article is available online.**

## 592 **Acknowledgement**

593 This work is supported by the National Natural Science Foundation of China through  
594 grants 41371478 and 41371453.

## 595 **References**

- 596 Adon, M., Galy-Lacaux, C., Delon, C., Solmon, F., and Tchente, A. T. K.: Dry  
597 deposition of nitrogen compounds (NO<sub>2</sub>, HNO<sub>3</sub>, NH<sub>3</sub>), sulfur dioxide and ozone  
598 in west and central African ecosystems using the inferential method, *Atmos.*  
599 *Chem. Phys.*, 13, 11351-11374, 2013.
- 600 Arneth, A., Schurgers, G., Hickler, T., and Miller, P. A.: Effects of species composition,  
601 land surface cover, CO<sub>2</sub> concentration and climate on isoprene emissions from  
602 European forests, *Plant Biol.*, 10, 150-162, 2008.
- 603 Arneth, A., Schurgers, G., Lathiere, J., Duhl, T. R., Beerling, D. J., Hewitt, C. N.,  
604 Martin, M., and Guenther, A. B.: Global terrestrial isoprene emission models:  
605 sensitivity to variability in climate and vegetation, *Atmos. Chem. Phys.*, 11,  
606 8037-8052, 2011.
- 607 Arya, S.P.: *Air Pollution Meteorology and Dispersion*. Oxford University Press, Inc.;  
608 New York, New York, 1999.
- 609 Ashworth, K., Wild, O., and Hewitt, C. N.: Sensitivity of isoprene emission estimated

610 using MEGAN to the time resolution of input climate data, *Atmos. Chem. Phys.*,  
611 10, 1193-1201, 2010.

612 Aydin, Y. M., Yaman, B., Koca, H., Dasdemir, O., Kara, M., Altiok, H., Dumanoglu,  
613 Y., Bayram, A., Tolunary, D., Odabasi, M., and Elbir, T.: Biogenic volatile  
614 organic compound (BVOC) emissions from forested areas in Turkey:  
615 Determination of specific emission rates for thirty-one tree species, *Sci. Total*  
616 *Environ.*, 490, 239-253, 2014.

617 Calfapietra, C., Fares, S., Manes, F., Morani, A., Sgrigna, G., and Loreto, F.: Role of  
618 biogenic volatile organic compounds (BVOC) emitted by urban trees on ozone  
619 concentration in cities: A review, *Environ. Pollut.*, 183, 71-80, 2013.

620 Camporn, S. J.: *Ecophysiological Responses of Plants to Air Pollution*, DOI:  
621 10.1002/9780470015902.a0003206.pub2, 2013. Available at <http://onlinelibrary.wiley.com/doi/10.1002/9780470015902.a0003206.pub2>.

622  
623 Central Government of China: Forest cover area from artificial afforestation in the  
624 Three Northern Regions Shelter Forest regions (in Chinese), 2012. Available  
625 at [http://www.gov.cn/jrzq/2012-08/27/content\\_2211594.htm](http://www.gov.cn/jrzq/2012-08/27/content_2211594.htm) .

626 Chang, K. H., Yu, J. Y., Chen, T. F., and Lin, Y. P.: Estimating Taiwan biogenic VOC  
627 emission: Leaf energy balance consideration, *Atmos. Environ.*, 43, 5092-5100,  
628 2009.

629 Chen, Y., Li, D. W., Shi, Y., and He, X.: Emission rate of biogenic volatile organic  
630 compounds from urban trees in Shenyang, China, *Journal of Northeast Forestry*  
631 *University*, 37, 47-49, 2009 (in Chinese).

632 Cheng, D., Gu, J.: Influence of the Three Northern Regions Shelter Forest on micro-  
633 scale climate. In: Zhu, T. (Ed.), *Ecological Benefit and Physical Characteristics*  
634 *of Atmospheric Boundary-layer of the Three Northern Regions Shelter Forest* (in  
635 Chinese), Meteorological Publisher of China, Beijing, pp. 209-216, 1992.

636 Chinese Environmental Protection Agency (1992) Action plans for implementing air  
637 pollution control strategy. Available at [http://www.zhb.gov.cn/gkml/hbb/bwj/201309/t20130918\\_260414.htm](http://www.zhb.gov.cn/gkml/hbb/bwj/201309/t20130918_260414.htm), in Chinese.

638  
639 Constable, J. V. H., Guenther, A. B., Schimel, D. S., and Monson, R. K.: Modelling  
640 changes in VOC emissions in response to climate change in the continental  
641 United States, *Global Change Biol.*, 5, 791-806, 1999.

642 Ding, Y., Li, Q., and Dong, W.: A numerical assessment of effect of forest coverage on  
643 regional climate in China (in Chinese), *J. Meteorol. Res.*, 63, 613-621, 2005.

644 Fang, J. Y., Chen, A. P., Peng, C. H., Zhao, S. Q., and Ci, L. J.: Changes in forest  
645 biomass carbon storage in China between 1949 and 1998, *Science*, 292, 2320-  
646 2322, 2001.

647 Fenn, M. E., Ross, C. S., Schilling, S. L., Baccus, W. D., Larrabee, M. A., and  
648 Lofgren, R. A.: Atmospheric deposition of nitrogen and sulfur and preferential  
649 canopy consumption of nitrate in forests of the Pacific Northwest, USA, *Forest*  
650 *Ecol. Management*, 302, 240-253, 2013.

651 Fensholt, R., Rasmussen, K., Nielsen, T. T., and Mbow, C.: Evaluation of earth obser-  
652 vation based long term vegetation trends—intercomparing NDVI time  
653 seriestrend analysis consistency of Sahel from AVHRR GIMMS, Terra MODIS

654 and SPOTVGT data, *Remote Sens. Environ.*, 113, 1886-1898, 2009.

655 Geron, C., Guenther, A., Greenberg, J., Karl, T., and Rasmussen, R.: Biogenic volatile  
656 organic compound emissions from desert vegetation of the southwestern US,  
657 *Atmos. Environ.*, 40, 1645-1660, 2006.

658 Guenther, A., Zimmerman, P., Klinger, L., Greenberg, J., Ennis, C., Davis, K.,  
659 Pollock, W., Westberg, H., Allwine, G., Geron, C.: Estimates of regional natural  
660 volatile organic compound fluxes from enclosure and ambient measurements, *J.*  
661 *Geophys. Res.-Atmos.*, 101(D1), 1345-1359, 1996.

662 Guenther, A., Hewitt, C. N., Erickson, D., Fall, R., Geron, C., Graedel, T., Harley, P.,  
663 Klinger, L., Lerdau, M., McKay, W. A., Pierce, T., Scholes, B., Steinbrecher, R.,  
664 Tallamraju, R., Taylor, J., and Zimmerman, P.: A global-model of natural volatile  
665 organic-compound emissions, *J. Geophys. Res.-Atmos.*, 100, 73-92, 1995.

666 Guenther, A., Karl, T., Harley, P., Wiedinmyer, C., Palmer, P. I., and Geron, C.:  
667 Estimates of global terrestrial isoprene emissions using MEGAN (Model of  
668 Emissions of Gases and Aerosols from Nature), *Atmos. Chem. Phys.*, 6, 181-210,  
669 2006.

670 Guenther, A. B., Jiang, X., Heald, C. L., Sakulyanontvittaya, T., Duhl, T., Emmons, L.  
671 K., and Wang, X.: The Model of Emissions of Gases and Aerosols from Nature  
672 version 2.1 (MEGAN2.1): an extended and updated framework for modeling  
673 biogenic emissions, *Geosci. Model Dev.*, 5, 1471-1492, 2012.

674 Guo, P. P., Guo, K. J., Ren, Y., Shi, Y., Chang, J., Tani, A., and Ge, Y.: Biogenic  
675 volatile organic compound emissions in relation to plant carbon fixation in a  
676 subtropical urban-rural complex, *Landscape and Urban Planning*, 119, 74-84,  
677 2013.

678 Hanna, S.R., and Strimaitis, D. J.: *Workbook of Test Cases for Vapor Cloud Source*  
679 *Emission and Dispersion Models*. Published by CCPS/AIChE, 1989, 345 East  
680 47<sup>th</sup> St., New York, NY 10017, 103 pp.

681 Hanna, S. R., Russell, A. G., Wilkinson, J. G., Vukovich, J., and Hansen, D. A.: Monte  
682 Carlo estimation of uncertainties in BEIS3 emission outputs and their effects on  
683 uncertainties in chemical transport model predictions, *J. Geophys. Res.*, 110,  
684 372-384, 2005.

685 Helmig, D., Daly, R. W., Milford, J., and Guenther, A.: Seasonal trends of biogenic  
686 terpene emissions. *Chemosphere*, 93, 35-46, 2013.

687 Hu, H., Wang, H., Lu, X., and Qiu, Z.: Assessment of influence of shelter forest on  
688 climate in arid and semi-arid regions in China, *J. Nanjing Forestry University*  
689 (Natural science), 25, 77-82, 2001 (in Chinese).

690 Klinger, L. F., Li, Q. J., Guenther, A., B., Greenberg, J. P., Baker, B., and Bai, J.:  
691 Assessment of volatile organic compound emissions from ecosystems of China, *J.*  
692 *Geophys. Res.*, 107(D21), 4603, doi:10.1029/2001JD001076, 2002..

693 Lamb, B., Guenther, A., Gay, D., and Westberg, H.: A national inventory of biogenic  
694 hydrocarbon emissions, *Atmos. Environ.*, 21, 1695-1705, 1987.

695 Li, L. Y., Chen, Y., and Xie, S. D.: Spatio-temporal variation of biogenic volatile  
696 organic compounds emissions in China, *Environ. Pollut.*, 182, 157-168, 2013.

697 Liu, Y. Q., Stanturf, J. A., and Lu, H. Q.: Modeling the potential of the northern China  
698 Forest Shelterbelt in improving hydroclimate conditions, *J. Amer. Water*  
699 *Resources Assoc.*, 44, 1176-1192, 2008.

700 Makkonen, R., Asmi, A., Kerminen, V. M., Boy, M., Arneth, A., Guenther, A., and  
701 Kulmala, M.: BVOC-aerosol-climate interactions in the global aerosol-climate  
702 model ECHAM5.5-HAM2, *Atmos. Chem. Phys.*, 12, 10077–10096, 2012.

703 Mao, D., Wang, Z., Luo, L., and Ren, C.: Integrating AVHRR and MODIS data to  
704 monitor NDVI changes and their relationships with climatic parameters in  
705 Northeast China, *Inter. J. of Appl. Earth Obser. Geoinformation*, 18, 528-536,  
706 2012.

707 Muller, J. F., Stavrakou, T., Wallens, S., and Smedt, I. D.: Global isoprene emissions  
708 estimated using MEGAN, ECMWF analyses and a detailed canopy environment  
709 model, *Atmos. Chem. Phys.*, 8, 329-341, 2008.

710 Myles, L., Heuer, M. W., Meyers, T. P., and Hoyett, Z. J.: A comparison of observed  
711 and parameterized SO<sub>2</sub> dry deposition over a grassy clearing in Duke Forest,  
712 *Atmos. Environ.*, 49, 212-218, 2012.

713 Nichol, J., and Wong, M. S.: Estimation of ambient BVOC emissions using remote  
714 sensing techniques, *Atmos. Environ.*, 45, 2937-2943, 2011.

715 Nowak, D. J., Crane, D. E., and Stevens, J. C.: Air pollution removal by urban trees  
716 and shrubs in the United States, *Urban Forestry & Urban Greening*, 4, 115-123,  
717 2006.

718 Nowak, D. J., Hirabayashi, S., Bodine, A., and Greenfield, E.: Tree and forest effects  
719 on air quality and human health in the United States, *Environ. Pollut.*, 193, 119-  
720 129, 2014.

721 Pacifico, F., Harrison, S. P., Jones, C. D., and Sitch, S.: Isoprene emissions and  
722 climate, *Atmos. Environ.*, 43, 6121-6135, 2009.

723 Pang, Q.: Construction of the Three Northern Regions Shelter Forest in China,  
724 Forestry Publisher of China, Beijing, 1992 (in Chinese).

725 Parungo, F., Li, Z., Li, X., Yang, D., and Harris, J.: Gobi dust storms and the Great  
726 Green Wall, *Geophys. Res. Lett.*, 21, 999-1002, 1994.

727 Penuelas, J., and Staudt, M.: BVOCs and global change, *Trends Plant Sci*, 15, 133-  
728 144, 2010.

729 Penuelas, J., Rutishauser, T., and Filella, I.: Phenology feedbacks on climate change,  
730 *Science*, 324, 887-888, 2009.

731 Pfister, G. G., Emmons, L. K., Hess, P. G., Lamarque, J. F., Orlando, J. J., Walters, S.,  
732 Guenther, A., Palmer, P. I., and Lawrence, P. J.: Contribution of isoprene to  
733 chemical budgets: A model tracer study with the NCAR CTM MOZART-4,  
734 *J. Geophys. Res.-Atmos.*, 113, 79-88, 2008.

735 Purves, D. W., Caspersen, J. P., Moorcroft, P. R., Hurtt, G. C., Pacala, S. W.: Human-  
736 induced changes in US biogenic volatile organic compound emissions: evidence  
737 from long-term forest inventory data, *Global Change Biol.*, 10, 1737-1755, 2004.

738 Sakulyanontvittaya, T., Duhl, T., Wiedinmyer, C., Helmig, D., Matsunaga, S.,  
739 Potosnark, M., Miford, J., and Guenther, A.: Monoterpene and sesquiterpene  
740 emission estimates for the United States, *Environ. Sci. Technol.*, 42, 1623-1629,

741 2008.

742 Sanderson, M. G., Jones, C. D., Collins, W. J., Johnson, C. E., and Derwent, R. G.:  
743 Effect of climate change in isoprene emissions and surface ozone levels,  
744 *Geophysical Research Letters*, 30, 159-171, 2003.

745 Sindelarova, K., Granier, C., Bouarar, I., Guenther, A. B., Tilmes, S., and Stavrakou,  
746 T.: Global data set of biogenic VOC emissions calculated by the MEGAN model  
747 over the last 30 years, *Atmos. Chem. Phys.*, 14, 9317–9341, 2014.

748 Situ, S., Wang, X., Guenther, A., Zhang, Y. L., Wang, X. M., Huang, M. J., Fan, Q.,  
749 Xiong, Z.: Uncertainties of isoprene emissions in the MEGAN model estimated  
750 for a coniferous and broad-leaved mixed forest in Southern China, *Atmos.*  
751 *Environ.*, 98, 105-110, 2014.

752 Song, Y. Y., Zhang, Y. Y., Wang, Q. G., An, J. L.: Estimation of biogenic VOCs  
753 emissions in Eastern China based on remote sensing data, *Acta Scientiae*  
754 *Circumstantiae*, 32, 2216-2227, 2012 (in Chinese).

755 Steiner, A., Luo, C., Huang, Y., Chameides, W. L.: Past and present-day biogenic  
756 volatile organic compound emissions in East Asia, *Atmos. Environ.*, 36, 4895-  
757 4905, 2002.

758 Stroud, C., Makar, P., Karl, T., Guenther, A., Geron, C., Turnipseed, A., Nemitz, E.,  
759 Baker, B., Potosnak, M., and Fuentes, J. D.: Role of canopy-scale  
760 photochemistry in modifying biogenicatmosphere exchange of reactive terpene  
761 species: Results from the CELTIC field study, *J. Geophys. Res.* 110, D17303,  
762 doi:10.1029/2005JD005775, 2005.

763 Tan, K., Piao, S., Peng, C., and Fang, J.: Satellite-based estimation of biomass carbon  
764 stocks for northeast China's forests between 1982 and 1999, *Forest Ecol*  
765 *Management*, 240, 114-121, 2007.

766 Tan, M., and Li, X.: Does the Green Great Wall effectively decrease dust storm  
767 intensity in China? A study based on NOAA NDVI and weather station data,  
768 *Land Use Policy*, 43, 42-47, 2015.

769 Turner, D. P., Wones, A. G., Pross, D., and Phillips, D. L.: Climate change and global  
770 isoprene emissions, Paper 91-126. 3, *Global Climate Change: Papers from the*  
771 *84th Annual General Meeting of the Air and Waste Management Association*,  
772 June 16-21, Vancouver, 1991.

773 Wang, Q., Zhang, B., Dai, S. P., Zou, Y., Ma, Z. H., and Zhang, Y. N.: Dynamic  
774 changes in vegetation coverage in the Three Northern Regions Shelter Forest  
775 Program based on GIMMS AVHRR NDVI, *Resour. Sci.*, 33, 1613-1620, 2011  
776 (in Chinese).

777 Wang, B., Shao, M., Lu, S. H., Yuan, B., Zhao, Y., Wang, M., Zhang, S. Q., and Wu,  
778 D.: Variation of ambient non-methane hydrocarbons in Beijing city in summer  
779 2008, *Atmos. Chem. Phys.*, 10, 5911–5923, 2010.

780 Wang, M., Shao, M., Chen, W., Yuan, B., Lu, S., Zhang, Q., Zeng, L., and Wang,  
781 Q.: A temporally and spatially resolved validation of emission inventories by  
782 measurements of ambient volatile organic compounds in Beijing, China,  
783 *Atmos. Chem. Phys.*, 14, 5871–5891, 2014.

784 Wang, Z. H., Bai, Y. H., Zhang, S. Y.: A biogenic volatile organic compounds

785 emission inventory for Beijing, *Atmos. Environ.* 37, 3771-3782, 2003  
786 Wei, X. L., Li, Y. S., Lam, K. S., Wang, A. Y., and Wang, T. J.: Impact of biogenic  
787 VOC emissions on a tropical cyclone-related ozone episode in the Pearl River  
788 Delta region, China, *Atmos. Environ.*, 41, 7851-7864, 2007.  
789 Yan, Q. L., Zhu, J. J., Hu, Z. B., and Sun, O. J.: Environmental impacts of the Shelter  
790 Forests in Horqin sandy land, Northeast China, *J. Environ. Qual.*, 40, 815-824,  
791 2011.  
792 Zeman K., and Brechler, J.: Emissions of biogenic VOC from forest ecosystems in  
793 central Europe: Estimation and comparison with anthropogenic emission  
794 inventory, *Environ. Pollut.*, 158, 462-469, 2010.  
795 Zhang, L., Moran, M. D., Makar, P. A., Brook, J. R., and Gong, S.: Modelling  
796 gaseous dry deposition in AURAMS: a unified regional air-quality modelling  
797 system, *Atmos. Environ.* 36,537-560, 2002.  
798 Zhang, X., Huang, T., Zhang, L., Gao, H., Shen, Y., and Ma, J.: Trends of deposition  
799 fluxes and loadings of sulfur dioxide and nitrogen oxides in the artificial Three  
800 Northern Regions Shelter Forest across northern China, *Environ. Pollut.*, 207,  
801 238-247, 2015.  
802 Zhang, Y., Wang, X., and Qin, S.: Carbon stocks and dynamics in the three-north  
803 protection forest program, China, *Austrian J. of Forest Sci.*, 130, 25, 2013.  
804 Zheng, X., and Zhu, J.: Estimation of shelter forest area in Three Northern Regions  
805 Shelter Forest Program region based on multi-sensor remote sensing data, *Chin.*  
806 *J. Appl. Ecol.*, 24, 2257-2264, 2013.  
807 Zhong, Z., Wang, H., Xiong, W., and Sha, W.: A numerical investigation of  
808 association between environment and the Three Northern Regions Shelter Forest:  
809 Model evaluation and verification, *J. PLA University of Technology*, 2, 7-12,  
810 2001 (in Chinese).

811

812 **The Supplement related to this article is available online**

### 813 **Figures captions**

814 **Figure 1.** The Three Northern Regions Shelter Forest (TNRSF) in Northern China.  
815 The Northwest China region of the TNRSF, defined by grey color, includes Xinjiang,  
816 Gansu, the north of Qinghai, Ningxia, West Inner Mongolia, and the north of Shaanxi;  
817 The Central-north China region, defined by orange gold color, includes the north of  
818 Shanxi and Hebei provinces, Beijing, Tianjin, and Central Inner Mongolia; The  
819 Northeast China region, defined by brass color, includes East Inner Mongolia, part of  
820 Liaoning, Jilin, and Heilongjiang provinces. Red, blue and yellow circles in the inner  
821 figure (right-lower corner of the figure) indicate three small areas in the TNRSF, a  
822 farmland, and the boreal forest from which isoprene emission flux are extracted for  
823 comparison (see Results and Discussions sections). Two megacities, Beijing and  
824 Tianjin in the Central-North China region, are also indicated.

825 **Figure 2.** Domain-averaged annual emission flux ( $\text{micro-moles m}^{-2} \text{ h}^{-1}$ ) of isoprene  
826 over the TNRSF from 1982 to 2010. Red dot line indicates linear trend of emission  
827 fluxes and shading stands for  $\pm 1$  standard deviation of emission fluxes.



828 **Figure 3.** Differences of emission flux ( $E_{2010} - E_{1982}$ , micro-moles  $m^{-2} h^{-1}$ ) of isoprene  
829 between 1982 and 2010. The emission fluxes in these two years are shown in Fig. S3a  
830 and b of Supporting Information

831 **Figure 4.** (a) Gridded annual isoprene biogenic emission (micro-moles  $m^{-2} h^{-1}$ ) in  
832 2000 over Northern China with spacing  $1/4^{\circ} \times 1/4^{\circ}$  latitude/longitude; (b) slopes of  
833 linear regression relationships between annual mean isoprene emission flux (micro-  
834 moles  $m^{-2} h^{-1}$ ) and the time sequence (or linear trend) from 1982 to 2010 across  
835 Northern China.

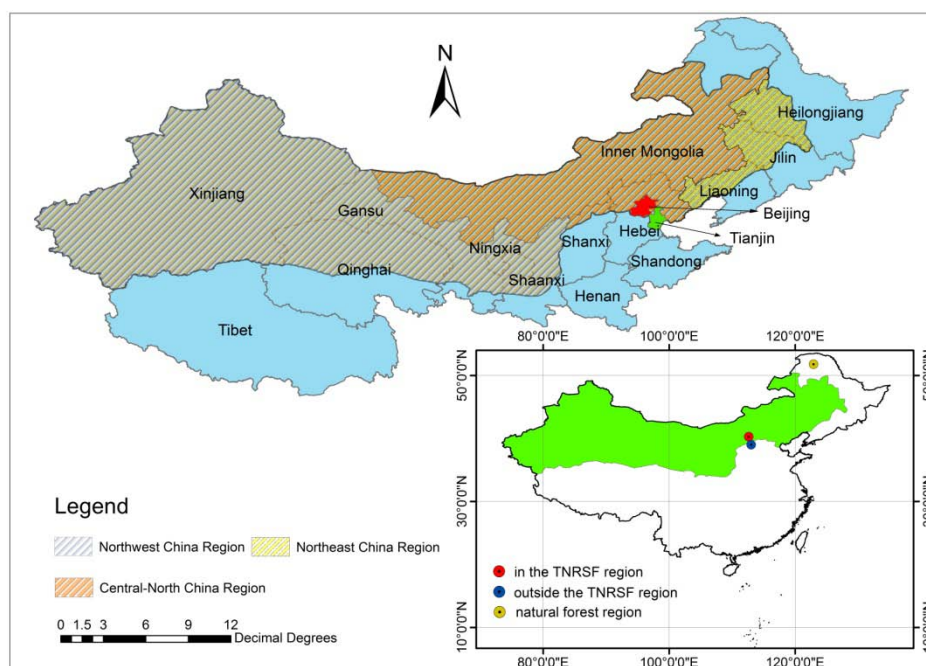
836 **Figure 5.** Slopes of linear regression relationships between summer mean isoprene  
837 emission flux (micro-moles  $m^{-2} h^{-1}$ ) and the time sequence (or linear trend) from 1982  
838 to 2010 across the TNRSF.

839 **Figure 6.** Annual variations of emission fluxes of isoprene averaged over three  
840 regions of the Northeast, Central-North, and Northwest China region of the TNRSF.  
841 Dotted straight line represent linear trend of isoprene emission fluxes in the Central-  
842 North China region.

843 **Figure 7.** Annual variation and trend of isoprene emission flux spatially averaged  
844 over three small areas in and outside the TNRSF in Central-North China and natural  
845 (boreal) forest region as marked in **Fig. 1**. The left-hand-side y-axis scales trend of  
846 isoprene emission fluxes in the TNRSF region and boreal forest in Northeast China  
847 and right-hand-side y-axis scale emission flux from the farmland outside the TNRSF.

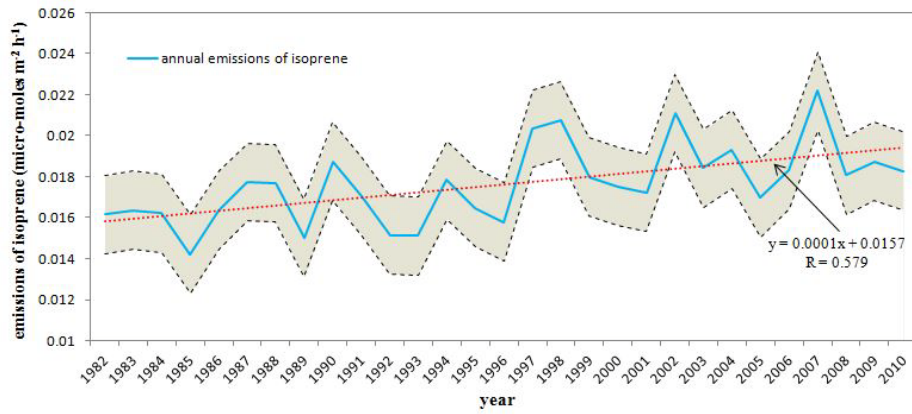
848 **Figure 8.** Measured ambient concentrations of TVOC ( $mg m^{-3}$ ) with frequency of 1  
849 min from 2 – 4 pm local time at 4 paired monitoring sites within and outside the  
850 TNRSF. (a) Langfang (August 9 2015), (b) Xinglong (August 10 2015); Zhangbei  
851 (North, August 12 2015), (c) Zhangbei (South, 13 August 2015).

852  
853



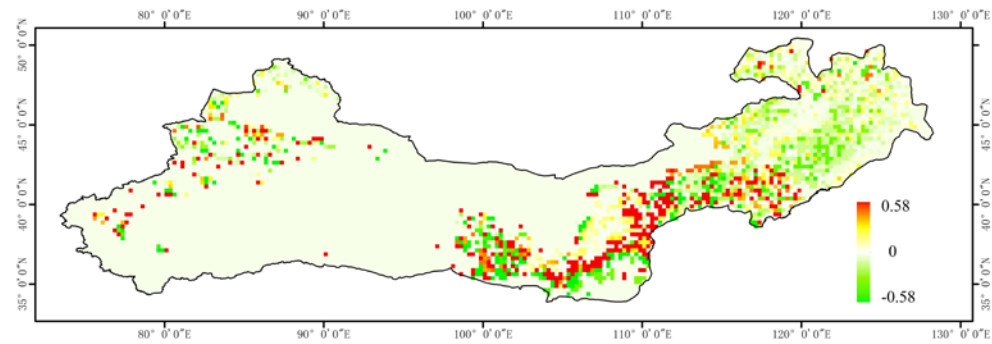
854  
855  
856

**Figure 1**



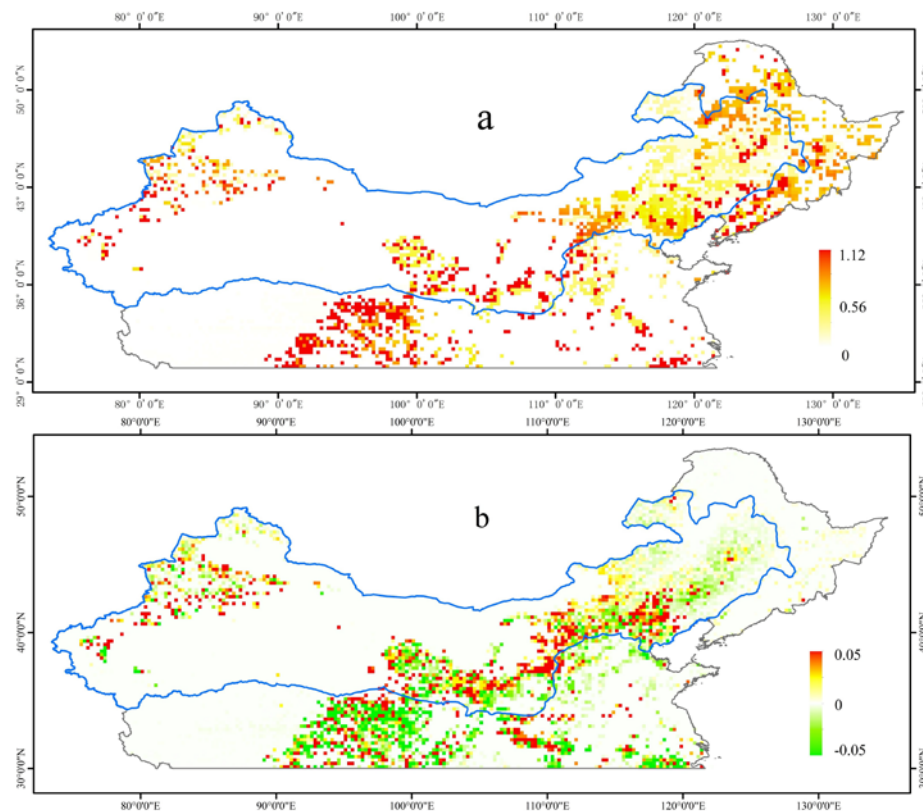
857  
858  
859

Figure 2



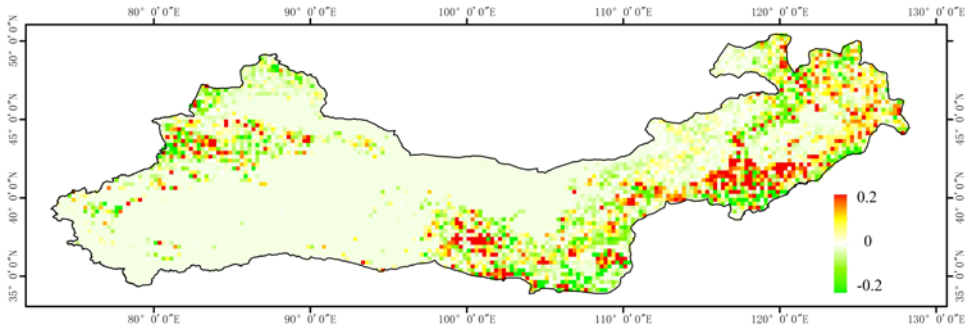
860  
861  
862

Figure 3



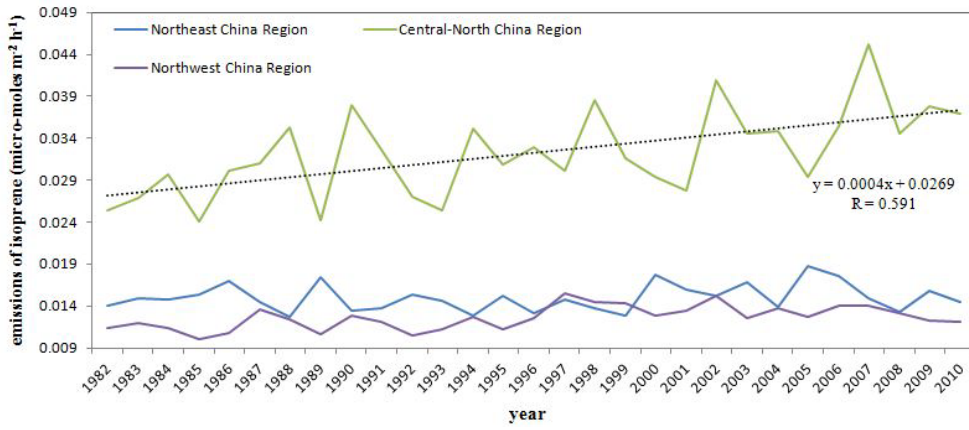
863  
864  
865

Figure 4



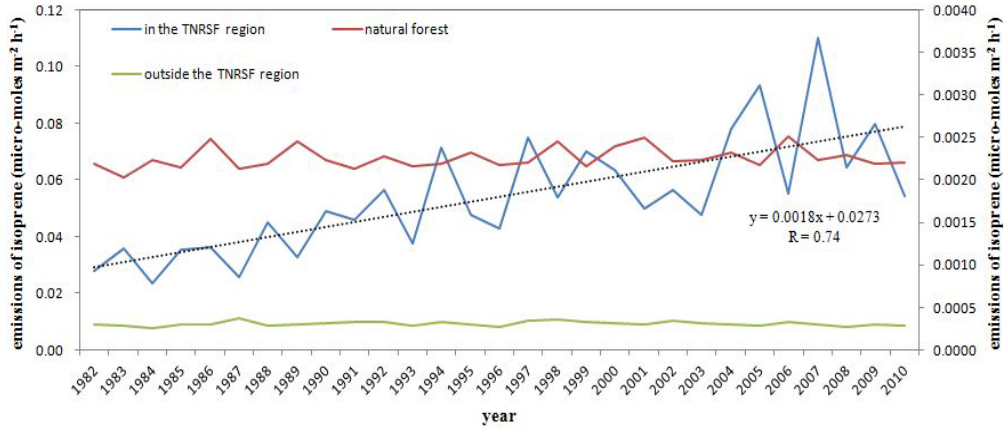
866  
867  
868

Figure 5



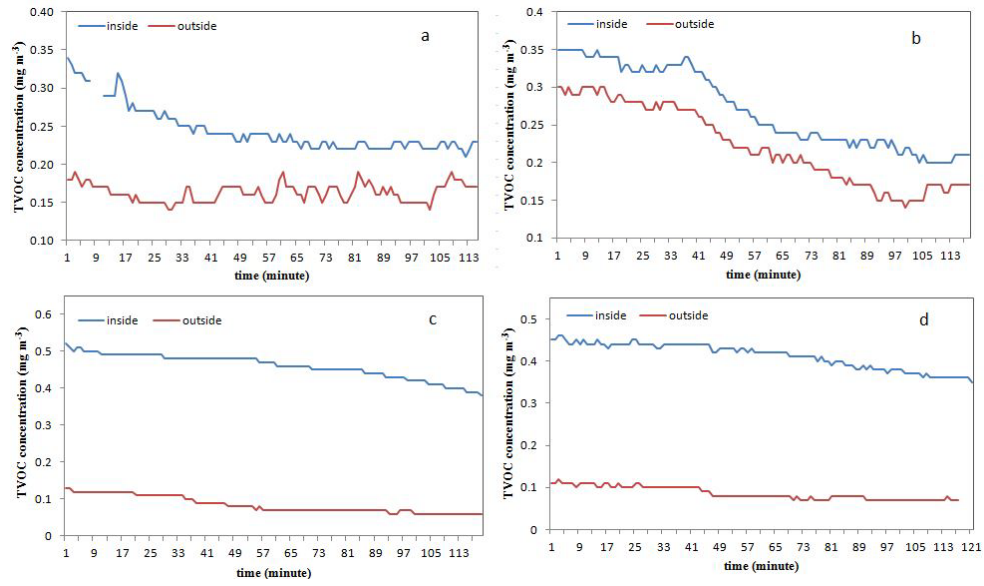
869  
870  
871

Figure 6



872  
873  
874

Figure 7



875  
876

Figure 8